Int. J. Rock Mech. Min. Sci. & Geomech. Abstr. Vol. 26, No. 6, pp. 647–660, 1989
Printed in Great Britain

0148-9062/89 $3.00 + 0.00
Pergamon Press plc

Some Problems in Estimating Horizontal Stress Magnitudes in "Thrust" Regimes

K. EVANS†
T. ENGELDER‡

Since hydraulic fractures exhibit a strong tendency to propagate in a plane normal to the least principal stress, the preferred plane of propagation under thrust *stress regime ($S_h > S_v$) conditions is horizontal. This can lead to complications in applying the hydrofracture stress measurement technique as horizontal fractures do not directly sample the horizontal stress field. Recent experiences in conducting measurements in* thrust *regimes have highlighted two problems that might be encountered. The first is the possibility of horizontal fracture initiation at the wellbore. The second relates to the seemingly common problem of deciding whether ISIPs which lie close to the estimated overburden reflect least horizontal stress levels (which happen to coincide with S_v) or vertical stress levels (resulting from fracture rotation to a horizontal plane in response to $S_h > S_v$). If the latter is true, then the ISIPs represent only lower bounds to the true values of S_h.*

We present two datasets which have bearing on the two problems noted above. In the first we review measurements conducted in a vertical borehole penetrating granite in which the vast majority of induced fractures were horizontal at the wellbore. Evidence suggests that these fractures were not a result of packer-induced stresses or incipient natural fractures but rather were a consequence of both high horizontal stress levels and fluid infiltration of the wellbore wall during the 15 sec of pump time required to attain breakdown. The absolute magnitudes of the horizontal stresses is not determined. However, through consideration of the elastic stress distribution about a vertical borehole it is possible, in principle, to estimate the horizontal stress difference $S_H - S_h$ from the horizontal fracture initiation pressure.

In the second dataset we present measurements conducted in three boreholes penetrating a sandstone/shale sequence in which the induced fractures were determined to be vertical at the wellbore. However, by modelling the anticipated effects of topography it is clear that the ISIPs above a certain stratigraphic horizon consistently reflect the vertical stress, and not S_h. *No evidence of dual shut-in pressures, which might provide a measure of the magnitude of the least horizontal stress in these beds, was observed. Neither did the form of the post-shut in pressure decline for these beds display any characteristics that might have served to distinguish them as horizontal fracture controlled. This example shows that the presence of a vertical fracture trace at the wellbore cannot be taken as proof that the ISIP reflects S_h.*

INTRODUCTION

The hydraulic fracturing stress measurement literature contains many examples of stress measurements conducted under "thrust regime" conditions; that is, at a point in a borehole where the least horizontal principal total stress S_h, acting outside the wellbore stress perturbation is greater than or equal to the vertical total stress, S_v. As hydraulic fractures exhibit a strong tendency to propagate in a plane normal to the least principal stress, the preferred plane of propagation under "thrust regime" conditions is horizontal. Consequently, since horizontal fractures do not directly sample the horizontal stress field, it is not at all obvious that the technique can be successfully applied under "thrust regime" conditions. That the hydraulic fracturing technique can work at all is reliant firstly on the tendency for pressurized

†Lamont-Doherty Geological Observatory, Columbia University, Palisades, NY 10964, U.S.A. Now at: Institut für Geophysik, ETH Hönggerberg, CH-8093 Zürich, Switzerland.
‡Department of Geosciences, The Pennsylvania State University, University Park, PA 16802, U.S.A.

boreholes to fracture axially. Assuming this is achieved, it is further reliant on the ability to propagate the fracture in the energetically-unfavoured vertical plane for sufficient distance from the wellbore that the ISIP recorded at the end of pumping reflects the closure stress across the vertical section of the fracture. The reported successes of many investigators in obtaining super-lithostatic S_h-profiles which show consistent trends with depth suggests that the hydrofracture technique can work under "thrust regime" conditions. However, there are several reported cases where it demonstrably has not. Of perhaps even greater concern are those cases where the observed ISIPs fall near the lithostat. Here a crucial judgement must be made as to whether the ISIPs reflect S_v or S_h. In this paper we discuss two examples which illustrate the potential difficulties. The first bears on the problem of horizontal rather than vertical fracture initiation. The second focuses on the problem of deciding whether near-lithostat ISIPs reflect S_v or S_h through discussion of an example where, despite evidence that only vertical fracture traces were present at the wellbore, it was possible to show that the ISIPs in fact reflected S_v and not S_h. We discuss the observations in as much as they reveal potential pitfalls of the technique and suggest methods for overcoming them.

N. CONWAY, NH—HORIZONTAL FRACTURE INITIATION IN GRANITE ROCK

Horizontal (i.e. transverse) fracture initiation at the wellbore has been observed in both strongly-bedded sedimentary rock [1,2] and crystalline rock [3–5]. Ideally, borehole pressurization serves to impart about the borehole an increasingly tensile hoop stress, but does not significantly affect the axial total stress. Hence, simple mechanical analyses of fracture initiation which are based on a conventional tensile strength failure criterion but which neglect fluid infiltration into the wellbore wall predict only the formation of an axial fractures, regardless of the *in situ* stress state. The effect of significant fluid infiltration of the wellbore wall was first studied by Haimson [6]. He concluded that transverse fracture initiation was possible, but only under conditions of exceptionally high horizontal stresses. Bjarnason *et al.* [7] have recently developed a theory of horizontal fracture initiation, based on a modified Hoek–Brown failure criterion, which hypothesizes that a state of absolute tension exists at the borehole wall prior to fracturing. Most field investigators, however, explain transverse fracturing as the result of pressurization and subsequent extension of a pre-existing macroscopic flaw not recognized in the interval selection survey [5] or from stress disturbance of the borehole wall near the ends of the packer seats [8,9].

Observations

Recently, we reported some observations which attest that transverse fractures can initiate without the help of macroscopic horizontal flaws or packer effects [10]. The observations derive from a series of 21 tests conducted to ~600 m in a 76-mm dia drill hole penetrating Conway granite near North Conway, NH. Test intervals free of natural macroscopic fractures were selected on the basis of a fracture log drafted from physical inspection of the core [11], and a conventional suite of pump cycles performed. The resulting "least ISIP" depth profile is shown in Fig. 1. A subsequent impression packer survey of 18 fractures showed that in all but one case a horizontal fracture was present, the exception showing an *en-echelon* dipping trace. In only one interval was a vertical trace recognized, which cut through and offset the horizontal trace, implying the latter formed as a secondary back-fracture. The other horizontal traces showed no evidence of vertical steps which might indicate the presence of "invisible" vertical fractures thereby suggesting that only horizontal fracture traces were present. An important observation was that the horizontal fractures formed mostly near the centre of the interval and hence could not have been initiated by stresses arising from packer end effects [8,9]. Further, an investigation of the mechanical action of the straddle packer suggested that it contributed an axial tensile stress of only ~0.06 MPa at the wall near the interval centre at breakdown [10,12].

Infiltration as an explanation of horizontal fracture initiation

The observations are best explained as the result of fluid infiltration of the wellbore wall during the ~15 sec of pump time required to raise interval pressure to breakdown levels. This time is not unusually long for hydrofracture operations, yet it is sufficient to permit substantial penetration of wellbore pressure for many crystalline rocks. For example, a coefficient of diffusivity of 0.55 cm²/sec results in the penetration of the 75%-of-wellbore-pressure contour to a depth of ~1 cm by this time [10]. The diffusivity of Conway granite has not been determined, although that for Westerly granite is

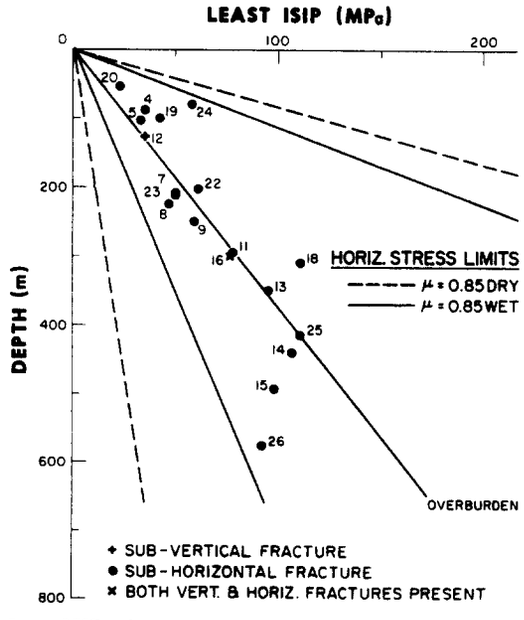

Fig. 1. Least ISIP values observed during the hydrofrac tests conducted in the N. Conway borehole. A density of 2.65 g/cm³ is assumed for the overburden.

Table 1

Dataset No.	Depth (m)	Pore pressure (MPa)	Overburden (MPa)	Breakdown (MPa)	ISIP (MPa)	$S_H - S_h$:over (MPa)	$S_H - S_h$:ISIP (MPa)
24	78.30	0.77	2.04	19.15	5.80	−1.97	5.55
4	87.90	0.86	2.29	16.30	3.60	2.26	4.89
19	99.10	0.97	2.58	9.45	4.25	11.91	15.25
5	103.00	1.01	2.68	16.10	3.30	3.22	4.46
22	201.20	1.97	5.23	15.80	6.10	8.08	9.82
7	208.85	2.05	5.43	18.80	5.05	4.43	3.67
23	211.55	2.08	5.50	23.40	5.00	−1.58	−2.58
8	223.50	2.19	5.81	9.00	4.60	18.16	15.74
9	250.50	2.46	6.51	14.90	5.90	11.52	10.30
10	265.00	2.60	6.89	17.00	—	9.38	—
11	293.70	2.88	7.64	21.55	7.75	4.62	4.85
18	311.75	3.06	8.10	22.90	11.05	3.64	9.53
13	351.70	3.45	9.14	24.40	9.50	3.45	4.17
25	414.55	4.07	10.78	20.35	10.80	11.71	11.76
14	441.72	4.33	11.48	18.95	10.60	14.81	13.05
15	492.25	4.83	12.80	16.90	9.70	19.84	13.65
26	579.12	5.68	15.06	16.80	9.15	23.92	12.11

0.22 cm²/sec [13]. Considering possible permeability enhancement from drilling damage, it is reasonable to suppose that by breakdown, connected porosity within at least 5 mm (and more likely 1 cm) of the borehole wall becomes pressurized to near wellbore pressure levels. The empirical effective stress law for tensile failure as determined by Jaeger [14] and used by Hubbert and Willis [15] will then apply. This predicts that horizontal fracturing will occur when the pore pressure in the wellbore wall P_p^{wall} exceeds the vertical total stress at the wall S_v^{wall} by the tensile strength T of the rock: that is:

$$P_p^{wall} \geq S_v^{wall} + T \quad (1)$$

and it is implicit that the penetration depth of significant pore pressure increase is sufficient to drive sub-critical cracks to instability. In order for horizontal fracture initiation to be realized requires that equation (1) be satisfied during wellbore pressurization before the conditions for axial fracture initiation are met. This imposes constraints between the two horizontal far-field stresses and the vertical stress in order that horizontal fracturing may be possible given infiltration. A general expression for the smallest value of S_h required for horizontal fracture initiation as a function of S_H, S_v, and the ambient pore pressure P_p is given by Evans *et al.* [10]. Using material properties appropriate for Westerly granite under 20 MPa confining pressure this relation becomes:

$$S_h \geq 1.3S_v - 0.1S_H - 0.2P_p + 0.75T, \quad (2)$$

which, for a biaxial stress field ($S_H = S_h$), reduces to:

$$S_H^b \geq 1.18S_v - 0.18P_p + 0.68T.$$

These relations imply that horizontal fracture initiation can occur where S_h is only modestly greater than the vertical stress, provided of course that pressure penetration is sufficient. These stress conditions were realized in the N. Conway hole [10].

Horizontal differential stress estimates from horizontal fracture initiation pressure

Although the absolute magnitude of S_H cannot be determined where horizontal fractures are initiated, it is possible to obtain an estimate of the value of the horizontal stress difference S_H–S_h, at least in principle. Haimson [6] gives an expression for the horizontal fracture initiation pressure $P_w^{H\text{-}frac}$, for a vertical hole penetrating a permeable medium subjected to arbitrary far-field stresses. After some rearrangement, his expression may be written:

$$S_H - S_h = \frac{1}{2\nu}\{S_v - (1-A)P_w^{H\text{-}frac} - AP_p + T\}, \quad (3)$$

where A is defined by:

$$A = \alpha\frac{(1-2\nu)}{(1-\nu)}.$$

We evaluated equation (3) using breakdown pressures observed in those N. Conway tests where fracturing initiated horizontally. Pore pressure was taken as hydro-

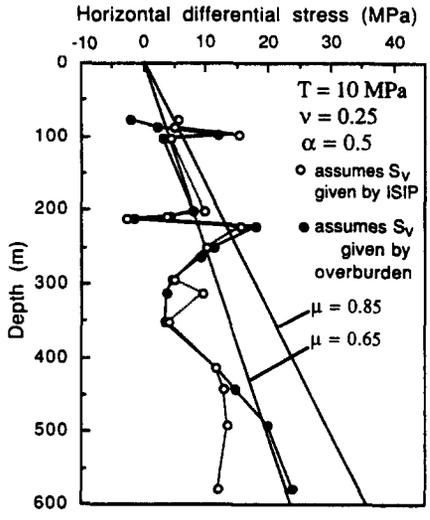

Fig. 2. Estimates of horizontal differential stress obtained from the pressure at which horizontal fractures initiated. The two values shown at each depth correspond to different S_v-estimates obtained from the computed overburden load and the observed ISIP. The diagonal lines define the maximum horizontal stress difference that can be supported by a cohesionless Coulomb material in which $S_h = S_v$.

static. A Poisson's ratio of 0.25, a Biot parameter α-value of 0.5 (appropriate for Westerly granite at 15 MPa confining pressure) and a tensile strength of 10 MPa were used [10]. The "far-field" vertical stress was estimated in two ways; firstly by assuming a value given by the weight of the overburden, and secondly by assuming a value given by the observed least ISIP. For horizontal fractures, the ISIP should be a direct local measure of S_v. The resulting estimates of $S_H - S_h$ are listed in Table 1 and are shown plotted as a function of depth in Fig. 2. Also shown are upper limits on admissible values of $S_H - S_h$ obtained by considering the bulk shear strength of the granite to be governed by a Coulomb friction law in a *thrust* stress regime. The limits are calculated from the relation (e.g. [16]):

$$S_H = S_v + 2\mu(S_v - P_p)\{(\mu^2 + 1)^{1/2} + \mu\}$$

and are plotted for values of the coefficient of sliding friction μ given by 0.65 and 0.85. Pore pressure is taken as hydrostatic. Note that because the failure lines are presented in terms of horizontal stress difference, they correspond as drawn to the specific case where $S_h = S_v$, which is the limiting case for "thrust" regime ($S_h \geq S_v$) conditions. They are thus upper bounds. In the case where S_h is strictly greater than S_v the predicted failure lines will lie to the left of those shown by the difference $S_h - S_v$. The estimates of $S_H - S_h$ in Fig. 2 which lie shallower than 300 m show greater scatter than might reasonably be expected. Two values (datasets 19 and 8 in Table 1) lie above the sliding friction limit while two (datasets 24 and 23) are negative and hence are non-physical. Estimates obtained below 300 m show greater consistency and are physically acceptable. This might be attributed to variability in tensile strength, the effects of which become less important at greater depth. It must be emphasized, however, that without independent corroborating evidence, the estimates of $S_H - S_h$ shown in Fig. 2 must be treated with circumspection. Equation (3) is derived from the assumption that fracture initiation occurs as soon as the net effective axial tension at some point about the fluid-infiltrated borehole wall reaches the tensile strength of the rock. Where an axis-normal deviatoric stress is present, this point will lie in the S_H direction. However, as Haimson [6] noted, although this condition may be satisfied at two opposite point localities at the borehole wall, macroscopic failure will not occur until the nucleating microfracture has attained some critical length, requiring growth into adjacent areas where the axial total stress is greater. The wellbore pressure at which macroscopic fracture extension occurs will thus be generally greater than the pressure $P_w^{H\text{-frac}}$, that features in equation (3), and the differential stress correspondingly underestimated. Evidence in support of this caution has been given by Enever [17] who observed partially-formed transverse fractures in an interval which ultimately fractured axially. Presumably stable transverse fracture growth was overtaken by unstable axial fracture growth as the wellbore pressure was increased. It would seem that if the method is to yield useful estimates of $S_H - S_h$ from observed horizontal fracture initiation pressure it will be for larger diameter boreholes where the axial stress "minimum" is not so strongly localized as in the 76 mm N. Conway hole.

An implication of this work for planning stress measurement campaigns in "thrust" stress regimes is that the inducement of an axial fracture cannot be taken for granted. The careful selection of an interval free of obvious horizontal "flaws" is not sufficient to ensure an axial fracture will be induced. Rather, the critical quantity is the pump time taken to attain breakdown. If our explanation is only qualitatively correct, the implication is that 15 sec can be too long, even for a granite which has a permeability of the order of 1 μdarcy. That horizontal fracture initiation is not routinely observed by other investigators working in "thurst" regimes with similar pump times might be accredited to sub-μdarcy permeabilities.

S. Canisteo, NY—vertical fracture initiation with horizontal fracture governed ISIPs

Despite the possibility of initiating horizontal fractures when $S_h > S_v$, it is evident from the literature that often purely axial fractures are initiated. This, however, does not necessarily guarantee a successful measurement. For if interpretable information is to be acquired about the magnitude of the horizontal stresses, it is necessary that the vertical attitude of the propagating fracture be maintained out to a sufficient distance from the wellbore such that the ISIP recorded upon termination of pumping is governed by the closure stress (that is, S_h) acting across this near-wellbore vertical section. If the fracture rotates into the horizontal plane at greater distance, then we might expect later portions of the post-shut-in pressure decline curve to be influenced by this remote horizontal attitude. Zoback *et al.* [18] have discussed this effect and define both an ISIP, which they presumed reflects S_h, and an asymptotic shut-in pressure (ASIP) which, they observe, frequently equals the vertical stress. Other investigators have observed two inflection points in the pressure decline curve which are taken to reflect closure stresses acting across vertical and horizontal sections of the induced fracture [2]. The distance out to which vertical fracture propagation must be maintained to ensure that an identifiable ISIP equal to S_h is obtained is an important question which is unlikely to have a simple answer. Mineback studies have shown that axial fractures initiated from boreholes oriented at awkward angles to the principal stresses quickly reorient themselves, usually within a few wellbore diameters, so as to propagate in a plane normal to the least principal stress [19]. Taken on face value, these observations suggest that in "thrust" stress regimes, the induced fracture should rotate to propagate horizontally within a few wellbore diameters. If such behaviour is common, then the practice of interpreting observed super-lithostatic (ISIPs) as a direct measure of S_h inherently presumes that the ISIP is governed by a "vertical" section which extends perhaps only several wellbore diameters, barely beyond the zone of wellbore-perturbed

stress. However short the requisite distance of vertical propagation may be, there remains the possibility that the fracture will rotate too quickly, or perhaps once rotated it will "back-fracture" to interect the wellbore, such as we observed at N. Conway. In these cases an ISIP equal to the vertical stress will be observed and the attempted measurement of the horizontal stress magnitudes fails to provide anything other than a lower bound to their true value.

There are many examples in the literature of measured S_h-profiles which lie close to the overburden, and each poses the question as to how we can know that "premature" fracture rotation did not occur, thereby relegating the stress estimates to lower-bound values. In cases where evidence of "back-fracturing" is recognized, there is little doubt that the ISIP merely reflects S_v. However, where only a vertical trace is observed at the wellbore, it is more difficult to decide. In what follows we describe an example where despite vertical traces at the wellbore, the spatial characteristics of the ISIP distribution strongly suggests the ISIPs reflect S_v and not S_h. After demonstrating this, we examine the data for insights into fracture propagation behaviour and discuss methods which might be used to overcome the problems associated with fracture rotation.

Observations

The measurements were made in three 200-mm dia uncased boreholes 1 km or so apart which penetrate horizontally-bedded Devonian sandstones and shales of the Appalachian Plateau in western New York [20]. More than 70 hydrofracture stress measurements were conducted to ~1 km depth. The wells are located on the side of a 230-m high hill (Fig. 3) with the *Wilkins* wellhead situated on the valley floor proximate to the village of South Canisteo, the *Appleton* wellhead located some 105 m higher at a distance of 1.4 km W–SW, and the westernmost, the *O'Dell* wellhead, situated a further 111 m higher, some 1 km due west of the Appleton. The stratigraphic section penetrated by the wells is shown in cross section A–A′ of Fig. 4. There is no vertical exaggeration. The stratigraphic features of note are the sand-rich beds, labelled as F through K (thickness < 13 m) and the Tully limestone which lies at ~1 km depth. Since bedding is essentially horizontal yet the wellhead heights differ, significant differences in vertical stress can be anticipated at common stratigraphic depths between wells.

Tested intervals were selected on the basis of televiewer logs. Test procedures are described in Evans *et al.* [20] and are typified by the test conducted at a depth of

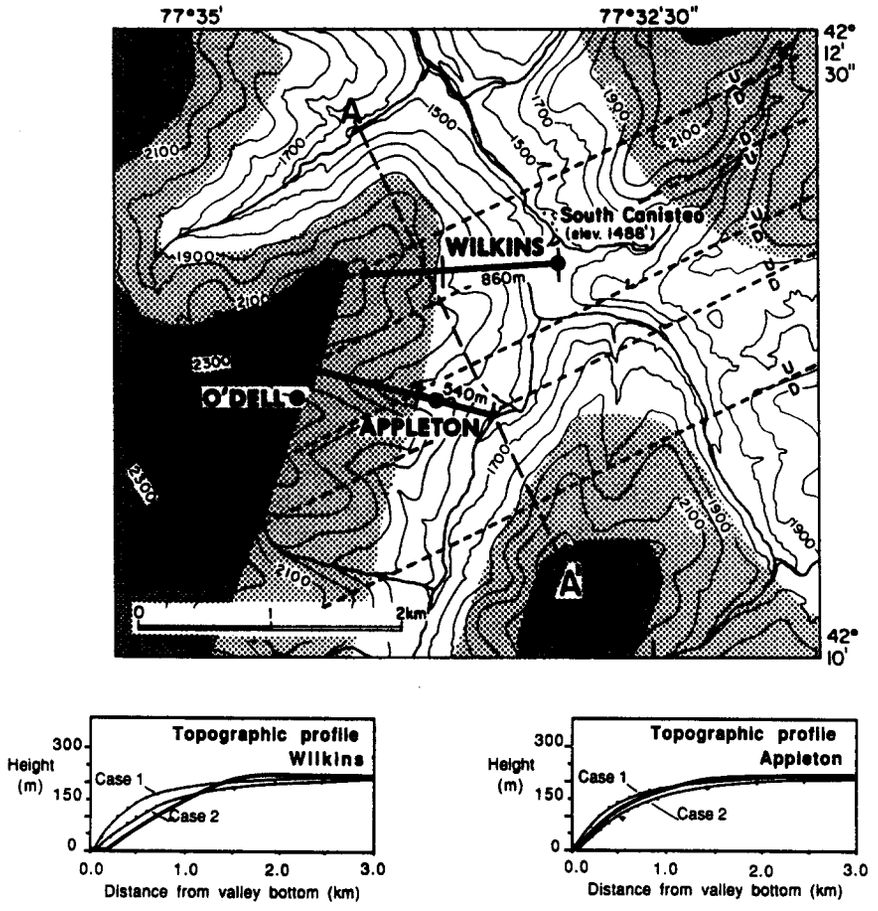

Fig. 3. Map of the S. Canisteo study area showing the location of the three wellheads with respect to topography in the area. The light and heavy stippled areas denotes regions higher than 1900 and 2200 ft, respectively, the bounding contours of which have been smoothed. The location of the two profiles shown at the foot of the figure is indicated. In estimating slope along these profiles, contours were smoothed in the same manner indicated by the stippled area boundaries. The theoretical profiles corresponding to the two models discussed in the text are also shown.

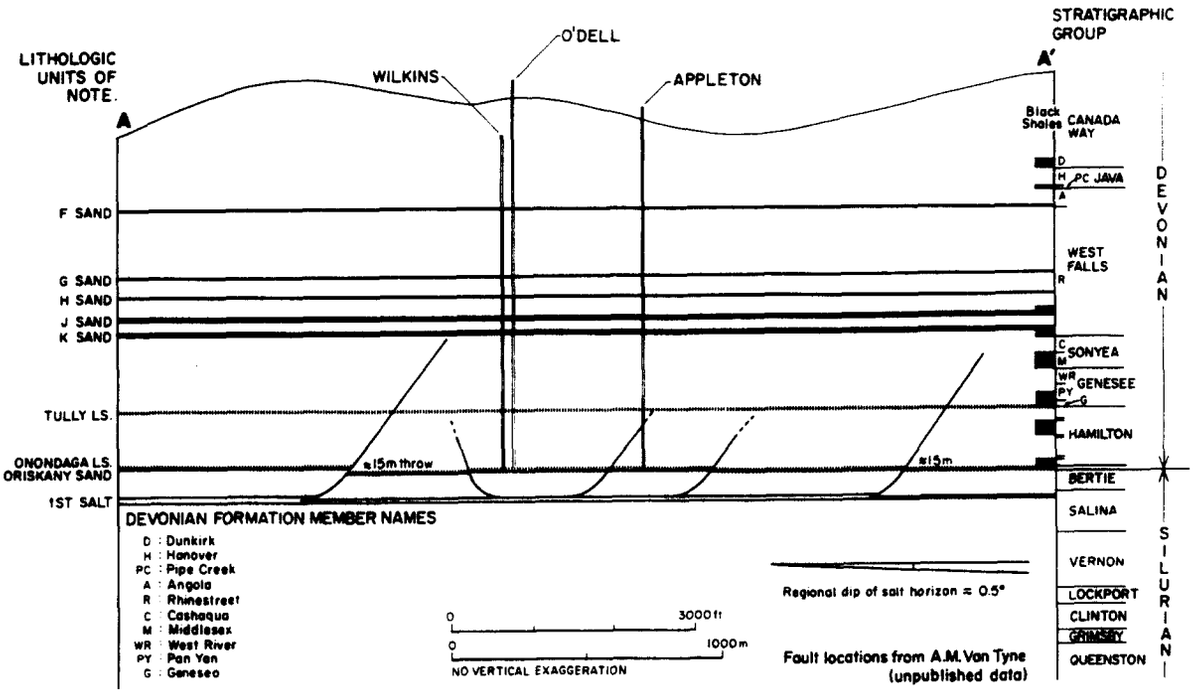

Fig. 4. Stratigraphic cross-section to profile A–A′ of Fig. 3. There is no vertical exaggeration. The wells have been projected onto the cross-section. The deepest stress measurement was conducted just below the Tully limestone.

486 m in the Wilkins well (dataset No. W2), the records from which are shown in Fig. 5. After the breakdown/shut-in/flow-back pump cycle, two 10 l "reopening" pump cycles were conducted followed by one or more 30–40 l pump cycles and occasional slow-pump or step-pump tests. In most reopen tests, time was not available to allow the fracture to fully drain before reopening. Hence the majority of intervals were reoccu-

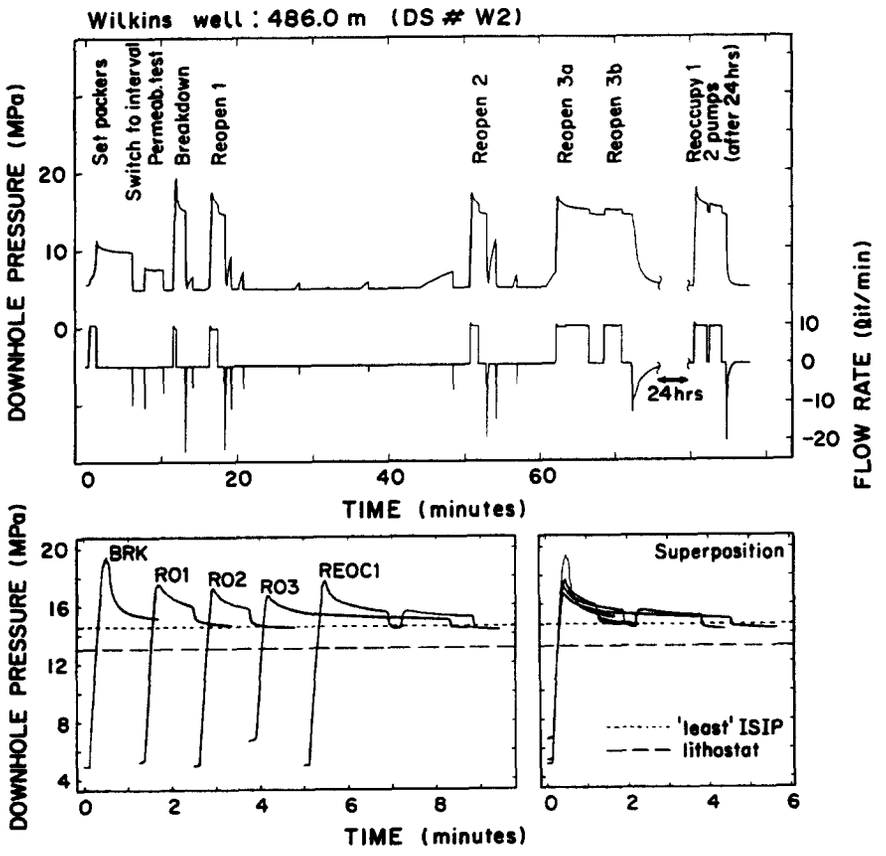

Fig. 5. Downhole pressure and flow rate records obtained during the testing of dataset W2 at 486.0 m depth in the Wilkins well. The test sequence is typical of the procedures used in the S. Canisteo wells.

pied between 6 hr and 8 days later and a reopen pump conducted with the fracture fully drained (referred to as a reoccupation pump). In the example shown, a period of 1 day elapsed between the initial test suite and the reoccupation. Following the pump tests, a televiewer survey was run to image the wellbore trace of the induced fracture. Immediately prior to this, an impression packer was set at each interval for 30 min at a pressure slightly less than the breakdown pressure to attempt to improve the definition of the fracture trace on the televiewer images. Vertical fracture traces were discernible in 70% of the intervals [20] with only one of the remainder being clearly horizontal [21].

Detail of pressure history during the pump cycles is shown on Fig. 5b. ISIPs were selected as the point at which the steep pressure decline immediately following shut-in departed from linearity (tangent method). No evidence of "dual closure" was found, despite plotting candidate decline curves on log–log plots. The resulting ISIP suites for each interval are listed in Table 2 and show that although values decline with successive pump cycles, in the vast majority of cases the final value was essentially attained at the end of the first reopening test. Later tests served only to improve the definition of the inflection point. An important result is that no systematic change in ISIP was observed during the later reoccupation pumps conducted between 6 hr and 8 days after the initial tests.

Interpretation of ISIPs—S_v or S_h?

Depth profiles of least ISIPs observed for each interval are plotted in Fig. 6. The depth axes have been shifted so that common stratigraphic horizons are aligned. The diagonal line represents the overburden load in each well as estimated from an integrated density log run in the Wilkins well. We observe that in each well the least ISIPs obtained above the H-sand define a quasi-linear trend which falls on or above the overburden trend. We refer to these as the "near-lithostat trends", and note that they exceed the overburden gradient by a factor of 1, 1.07 and 1.16 for the O'Dell, Appleton and Wilkins wells, respectively. Least ISIPs recorded in all sands and limestones below the H-sand fall on the extrapolation of these trends, but those for shales are lower. The question of interest here is whether the trends define the S_v-profile in each well rather than S_h. To address this question we exploit the 3-D description of ISIP variation afforded by having data from three boreholes. Two aspects of this distribution are noteworthy. Firstly, below the K-sand, ISIPs measured at common stratigraphic levels are the same in each well, despite the difference in overburden [20]. Secondly, the near-lithostat trends differ systematically between wells.

Both the above aspects provide a basis for discrimination between S_h and S_v in the presence of topography. To show this we employed a 2-D plane strain model given by Savage *et al.* [22] to compute the spatial variation of gravity-induced stresses resulting from the erosion of a long symmetric valley into an idealized elastic laterally-confined half-space. Although the 2-D model does not ideally represent the 3-D topography in the study area, it provides a reasonable semi-quantitative approximation. Two model topographic profiles are considered which are shown at the foot of Fig. 3. Profiles characterizing slopes in the vicinity of the Wilkins and Appleton wells are also shown for comparison. Short wavelength variations in topography are smoothed. Details of the modelling are presented in the Appendix and the results are depicted in Fig. 7 where we show predicted contours of vertical stress (right) and valley-normal horizontal stress (left) for the two model profiles. We see that below a few hundred metres depth, the lateral variation in valley-normal horizontal stress at a given stratigraphic level is small, whereas the corresponding lateral variation in vertical stress mimics the topographic profile, although less so at depth. The valley-parallel horizontal stress magnitudes are given by the plane strain relation $\sigma_y = \nu(\sigma_x + \sigma_v)$. Hence these contours (not shown) are also deflected downwards, but by a small fraction of the deflection to the vertical stress. Thus this simple model predicts that ISIPs which reflect S_h should be similar at common stratigraphic levels in the three wells, as we observe below the K-sand. Whether this result is useful in interpreting data from multiple holes depends upon the characteristic wavelength of the local terrain, the depth of the wells, and also the lateral uniformity of the strata. Lateral variations in material properties, such as due to dipping beds or structural discontinuities, will generally give rise to substantial lateral variations in horizontal stress magnitudes [23,24]. Thus, although recognition of lateral uniformity in an ISIP distribution obtained where there is significant topography can be taken to imply that the ISIPs measure S_h, the absence of lateral uniformity does not necessarily demonstrate otherwise. For the case in hand, we may have confidence that the ISIPs measured below the K-sand, with the exception of the Tully limestone, reflect S_h.

The systematic variation in the gradients of the near-lithostat trends is also reasonably well-explained by the model as reflecting S_v. In Figs 8a and b we show the predicted S_v depth profiles for the Wilkins and Appleton wells, respectively. Also shown is the overburden trend as computed from the density log (i.e. $\rho g d$ where d is the depth below the wellhead), and all ISIPs which define the near-lithostat trends (denoted in Table 2 by an asterisk). For model "case 1", the Wilkins ISIPs fall precisely on the predicted S_v-profile, but for the Appleton well the predicted S_v-profile does not differ significantly from the overburden. The model topography, however, is much steeper than applies to either of the two wells. For "case 2", which constitutes our overall best-fit model, the model topographic profile matches the Appleton profile well, although it is still somewhat steeper than the Wilkins. The predicted S_v-profile for the Wilkins well is a little higher than the ISIP trend, but not greatly so. For the Appleton well, the gradients of predicted S_v and observed ISIP are 1.02 and 1.07 times overburden, respectively. For the O'Dell well, the predicted S_v-gradient corresponds essentially to the overburden in both cases, as do the ISIPs. Thus, qualitatively if not

Table 2. Wilkins Well

Dataset No.	Depth (m)	Reopen 1 ISIP (MPa)	Reopen 2 ISIP (MPa)	Reopen 3 ISIP (MPa)	Reopen 4 ISIP (MPa)	Reoccupy 1 ISIP (MPa)	Reoccupy 2 ISIP (MPa)	Slow pump	Selected ISIP (MPa)
W43*	186.0	6.55	6.35	6.05					6.05
W42*	188.5	6.7	6.25						6.25
W41*	194.5	6.8	6.25	6.05					6.1
W40*	198.5	7.1	6.7	6.45	6.35				6.45
W1*	203.5	6.85	6.50	6.50	6.4	6.05* (16 hr)	6.5* (6 days)		6.4
W5*	207.0	7.0	6.9	6.7		6.65 (7 days)			6.7
W20*	252.7	8.3	7.95	7.75		9.25 (2 hr)	8.3 (15 hr)		7.75
W21*	257.2	8.5	8.4	8.15		7.85 (4 hr)	8.05 (1 day)		8.1
W22*	266.0	8.0	7.8	7.75		7.8 (1 day)			7.75
W4*	342.0	10.75	10.4	10.75		10.3 (8 days)			10.5
W23*	386.0	11.75	11.5	11.45					11.45
W3*	420.0	14.0	13.55	13.35					13.35
W2*	486.0	15.1	14.85	14.45	14.4	14.4 (1 day)			14.4
W30*	501.4	15.7	15.55	15.15		15.45 (1 day)			15.15
W39	560.5	17.55	16.35	16.05		16.9/16.35(2 days)			16.05
W14	579.0	16.95	17.0	17.2				17.2	17.2
W10*	582.5	18.75		18.2		18.0 (1 day)			18.2
W24	592.4	16.4	16.35	16.7					16.5
W25*	597.4	18.95	18.65	18.3					18.3
W38	621.8	19.8	18.9	18.85					18.35
W26	652.2	17.2	17.15	16.9					17.0
W27*	662.5	21.5	20.8	20.55					20.6
W28*	674.0	21.7	20.9	20.8					20.6
W29	680.0	19.15	19.3	19.1/19.1					19.1
W6	692.0	18.6	18.2	18.5/18.7		18.5 (2 days)			18.5
W31*	707.5	22.85	22.4	21.95					21.95
W15*	712.5	23.65	22.7	21.85		22.0 (7 days)			21.85
W16	724.0	16.35	15.8	15.6					15.6
W17	729.0	15.6	15.5	15.35		15.4 (7 days)			15.4
W18	747.0	16.25	15.95	15.8		16.05 (7 days)			19.95
W37	778.15	16.45	16.05			16.05 (1 day)			16.05
W19	832.5	17.55	17.35	17.0		17.0 (6 days)			17.0
W32	840.0	16.8	16.65	16.25		16.4 (10 hr)			16.25
W33	860.5	17.65	17.2	17.05		16.95 (7 hr)			17.05
W9	889.5	19.05	18.75	18.5		18.9 (8 days)			18.5
W34	951.0	20.55	20.35	20.2		20.25 (6 hr)			20.2
W35	960.5	20.2	20.05	20.15		19.95 (4 hr)			20.0
W36	977.6	21.0	21.0	20.85		20.85 (3 hr)			20.85
W7	985.5	20.3	20.05	19.9		20.25 (8 days)		19.9	19.9
W8	991.15	19.75	19.75	19.7		19.8 (1 day)			19.7
W12*	1009.5	31.85	30.6	30.6		31.0 (7 days)			30.6
W11	1013.5	24.55	24.6	24.45		24.25 (7 days)			24.45
W13	1037.15	21.95	21.85	21.8					21.8

Appleton Well									
A1*	186.7	5.5	5.55			5.35	5.4/5.35		5.35
A2*	230.0	6.6	6.5	6.5	6.5			6.8/9.5	6.6
A3*	248.3	7.8	7.5	7.6				7.6	7.5
A4*	277.3		8.35	8.15	8.0				8.0
A6*	293.8	9.5	9.05	8.9	9.1			13.3	9.0
A7*	304.8	11.0	10.9	10.65	10.45				10.5
A8*	311.85	10.55	10.65	10.4				9.7	10.4
A9*	356.35	11.2	10.3	10.05	9.9				10.0
A10*	365.85	10.95	10.65	10.65	10.65			16.4	10.65
A11*	374.1	11.15	10.85	10.8	10.6				10.6
A12*	440.5	13.05	12.75	12.9	12.45	12.6 (1 day)			12.5
A13*	527.25		14.65	14.85	14.65				14.65
A14*	677.15	18.2	18.1	18.4	18.3				18.3
A15	700.15	16.5	17.0			18.3 (1 day)			18.3
A16*	704.15	20.0	20.35	19.95	19.2				19.2
A17	748.15	18.1	18.5	18.3					19.2
A18*	770.65	22.45	22.05						22.05
A19*	778.15	22.8	22.05			21.85 (1 day)			22.05
A20	787.65	21.4	20.3	20.1					20.1
A21	833.6	15.9	15.75	15.9					15.9
A22	926.55	16.6	16.55	16.4					16.4
A23	999.55	20.15	19.8	19.65	19.6				19.6
O'Dell Well									
OD1*	246.75	8.45	8.05	7.5		7.5 (15 days)	7.9 (1day)		7.5
OD3*	342.0	9.65	9.4	9.4		9.3 (2 days)			9.3
OD2*	428.25	11.75	11.6	11.35		11.8 (2 days)			11.4
OD10	864.5	20.6	20.6	20.55					20.6
OD9*	896.5	24.85	25.05	24.45					24.5
OD8	909.5	20.35	19.7	19.6					19.5
OD7	922.5		21.15	20.05					20.0
OD4*	931.0	23.7 (?)				26.6/25.0/25.0 (2 day)	24.8/24.2 (1 day)		24.2
OD6	942.0	21.4	19.5/19.7/19.4	18.2				17–18	18.2
OD5	950.2	16.4	16.1	16.2					16.2

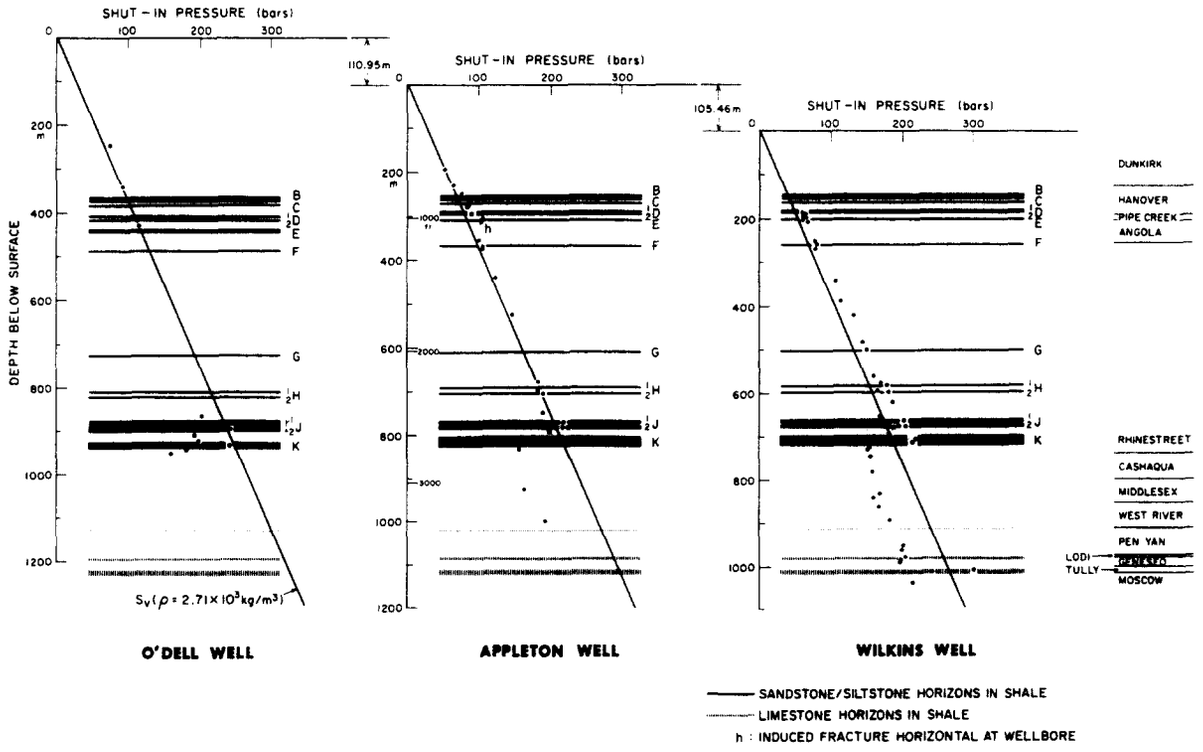

Fig. 6. ISIPs obtained in each of the three wells. The depth axes have been shifted so that common stratigraphic horizons are aligned. The location and thickness of the quartz-rich and limestone beds is indicated. The diagonal line represents the overburden as estimated by integrating the bulk density log and is not necessarily the same as the vertical stress.

precisely quantitatively, the near-lithostat trends correspond reasonably well to the predicted form of the S_v-profiles. That the fit is not precise might be accredited to the coarse 2-D representation of 3-D topography, and perhaps also to the possibility that ISIPs from horizontal fractures may slightly underestimate S_v, as suggested by Haimson *et al.* [2].

Discussion

The modelling results thus unequivocally suggest that the ISIPs which lie in the near lithostat trends measure S_v and not S_h, and hence are governed by the closure of a horizontal fracture. Yet we are fairly confident that in most cases only a vertical fracture trace was present at the wellbore. The post-fracture televiewer survey showed only vertical traces, but this alone cannot discount the possible presence of horizontal traces since they are notoriously difficult to detect on televiewer images from horizontally-bedded strata. Fortunately, evidence that "back-fracturing" was not common arose from our practice of setting an impression packer in each interval for 30 min prior to the post-frac televiewer survey. Upon bringing the packer to the surface after impressing all fractures shallower than 440.7 m (dataset No. A12) in the Appleton well, the packer was found to be decorated with vertical traces with only one horizontal trace visible. This suggests the majority of the induced fractures where wholly vertical at the wellbore and rotated to the horizontal plane after propagating some distance from the wellbore. An implication is that the absence of a horizontal fracture trace cannot be taken as proof that the ISIP reflects S_h.

In reasoning how far the vertical section of the fracture extended before turning, we might consider some implications of the fracture trace images described fully in Evans *et al.* [20]. Fracture extension around the packer seats was common, and occurred in most of the tests below the K-sand. Moreover, it is certain that these fractures were conducting substantial flow around the packers to the low-pressure wellbore during pumping, yet this did not effect the observed ISIPs which, by virtue of their lateral uniformity, almost certainly measure S_h. Thus, the fracture acts as an efficient valve and the ISIPs must be governed by fracture-normal stress acting within 1 m (the packer seal length) of the interval. Given this observation, it is difficult to see, in the case of fracture rotation, how an ISIP can be governed by the value of S_v if the vertical section of the fracture extends more than 1 m. Therefore, we suggest that rotation was very rapid, most likely within a few wellbore diameters, which is consistent with the mineback observations of Warren and Smith [19]. This also offers an explanation of why we do not observe a higher ISIP reflecting the closure of the vertical section of the fracture, since it is confined to the immediate vicinity of the wellbore and is of insufficient extent to act in the manner of a valve. Such rapid rotation to the horizontal plane will diminish whatever influence the vertical section may have on the pressure decline following shut-in and does not favour the development of inflectional features which reflect S_h, such as suggested by Zoback *et al.* [18].

Several authors have remarked that post-shut-in pressure decline curves from horizontal fractures display a characteristic signature of rapid decent to a sharp knee

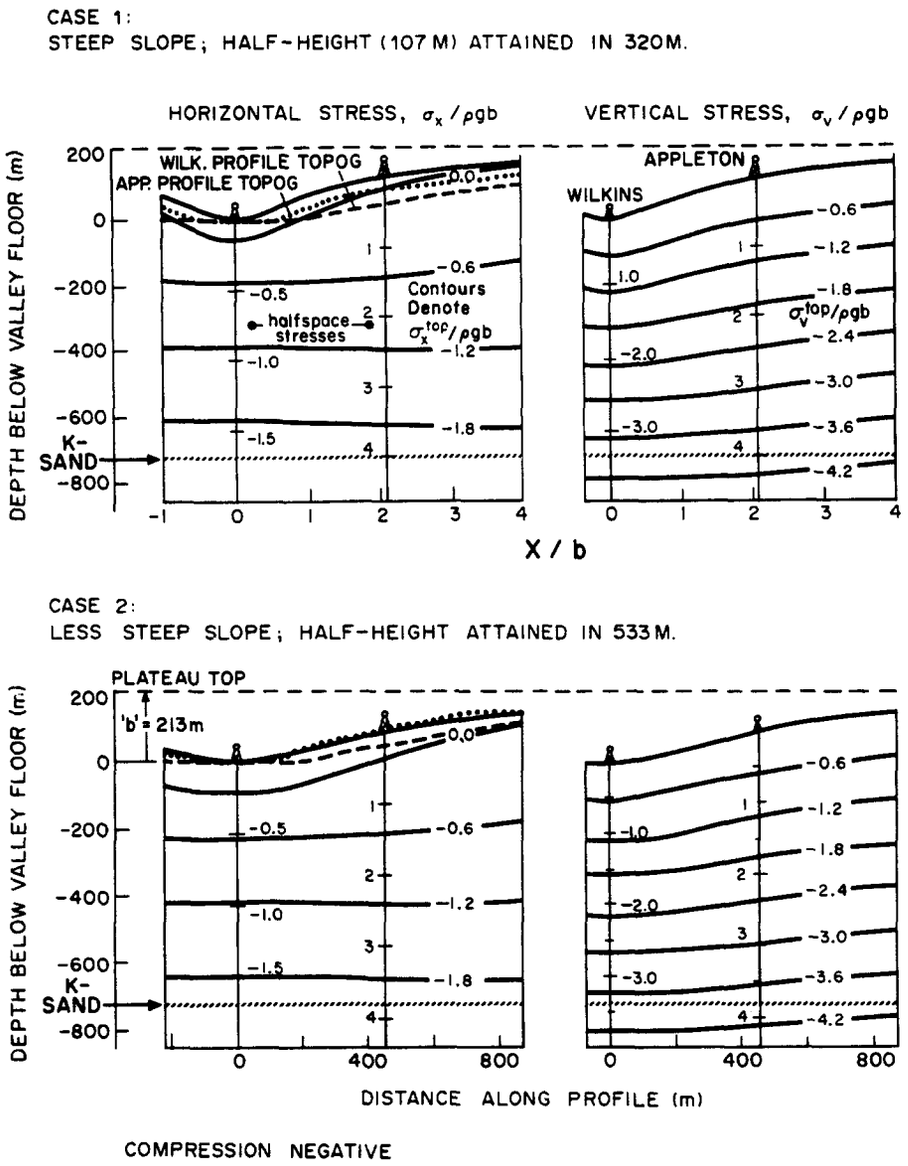

Fig. 7. Results of topographic stress modelling for a Poisson's ratio of 0.33 and a density of 2.71 g/cm^3 (after Savage *et al.*[22]) corresponding to the two profiles shown in Fig. 3. All depths are normalized by b, the asymptotic plateau height above the valley floor, of 213 m. All stress magnitudes are normalized to ρgb and hence must be multiplied by 5.66 to obtain values in MPa. Horizontal stress magnitudes (left figures) are essentially laterally uniform at stratigraphic horizons deeper than 300 m below the valley floor. Vertical stress (centre figures) increases with depth below the valley floor at a rate faster than the "overburden" which is defined for each well by the graduations along the well profile.

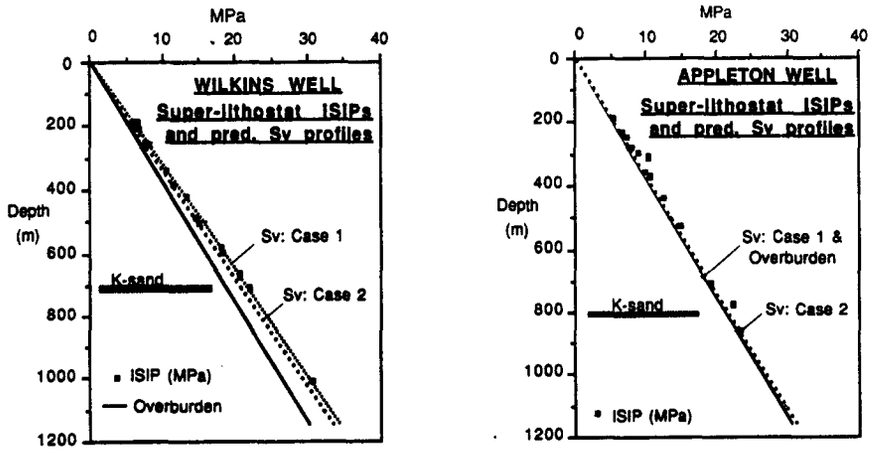

Fig. 8.(a) Predicted depth profiles of vertical stress for the Wilkins well for profile cases 1 and 2 of Fig. 7 together with the overburden and ISIP data points which fall on the near-lithostat trend; (b) same as Fig. 8a but for the Appleton well.

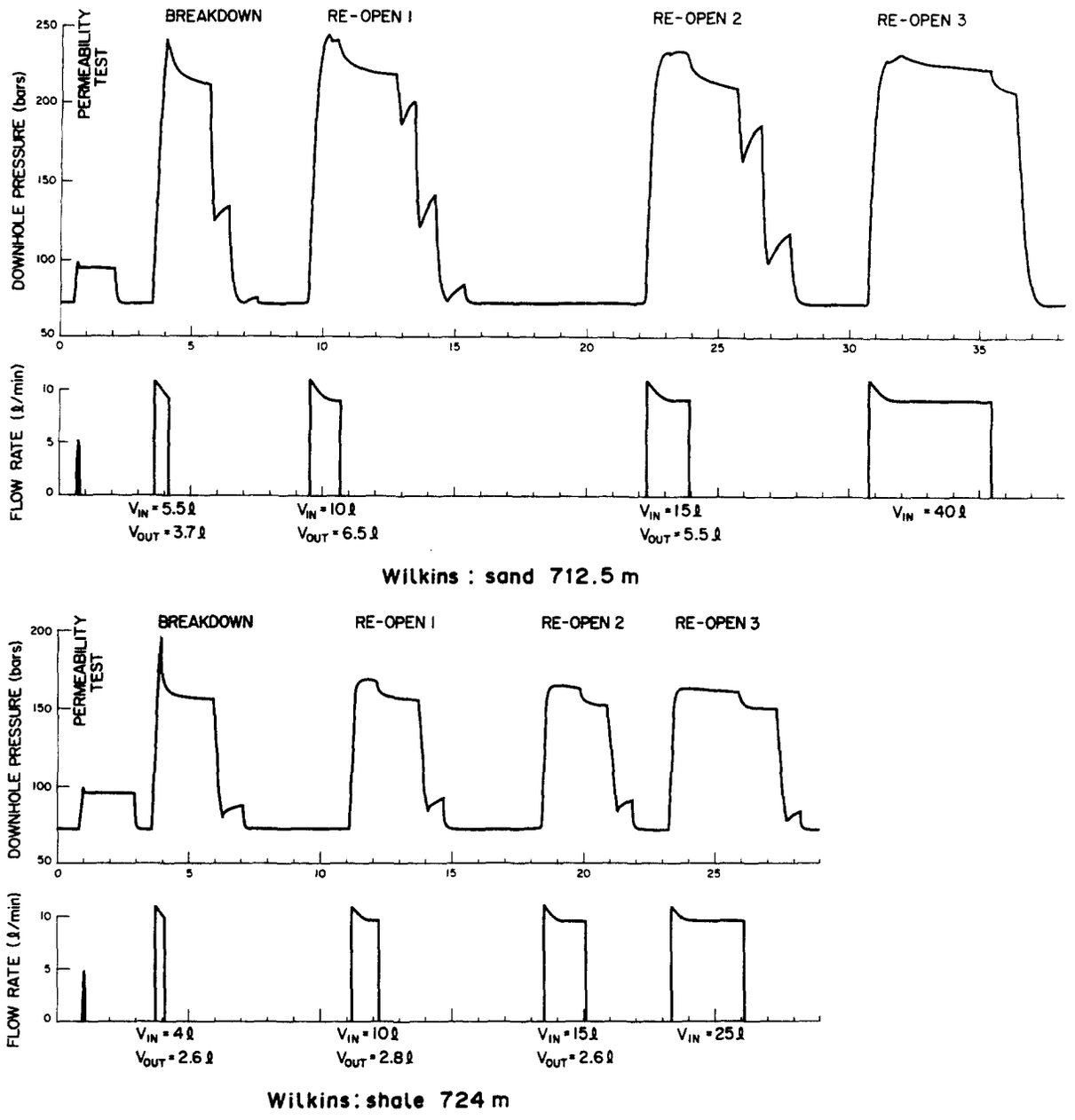

Fig. 9. Pressure and injection-rate records obtained during two tests; one conducted in the K-sand and the other in the immediately underlying shale. Note the difference in pumping pressures even though the intervals are only 10 m apart. The form of the post-shut-in pressure decline curves, however, are similar.

followed by a plateau at about the level of the vertical stress [2,4]. In Fig. 9 we show the records from the initial testing of two neighbouring intervals in the Wilkins well. The upper figure is for the K-sand, where we believe the ISIP of 22 MPa reflects S_v, the value of S_h being somewhat higher. The lower figure is for the shale immediately below the K-sand, where the ISIP of 15.6 MPa measures S_h. The forms of the post-shut-in pressure decline curves for the sand and shale are similar despite the evidence that they are predominantly governed by horizontal and vertical fractures, respectively. Furthermore, in the former test there is no indication of the pressure levelling off at the value of the vertical stress, an observation that holds true for most of the tests where the ISIP reflected S_v. Thus we are unable to discriminate between ISIPs which reflect S_h and S_v on the basis of post-shut-in pressure decline. We speculate that post-shut-in pressure decline behaviour which is diagnostic of S_v-governed ISIPs may be limited to cases where the horizontal fracture intersects the interval, which is not the case here.

Both Roegiers *et al.* [1] and Haimson *et al.* [2] have reported measurements in shales of the Appalachian Plateau which were subject to similar "thrust regime" conditions as those discussed here. Impression packer surveys showed horizontal fractures to be prevalent in both studies. Despite this, however, estimation of S_h was possible in both cases due to the identification of two inflexion points in the post-shut-in pressure decline curves, the first being interpreted as a measure of S_h and the second corresponding closely to the computed overburden. In order to observe such dual-closure phenom-

ena, it is essential that the downhole wellbore pressure significantly exceed the value of S_h during pumping. Roegiers *et al.* [1] allude to the use of viscous pumping fluids, presumably to promote high wellbore pressures and ensure fluid penetration of a vertical fracture, even though a horizontal fracture may be the principal conduit of fluid transport from the wellbore. In the measurements discussed here, pumping pressures were typically 1 MPa or so higher than the ISIP (Figs 5 and 9). If we suppose for the moment that horizontal "back-fracturing" was the rule, then since the likely magnitude of S_h in the K-sand is at least 24 MPa [25], the pumping pressure would have been insufficient to inflate the vertical fracture segment. In this case, pump-rates higher than our limit of 10 l/min or the use of more viscous fluids may have been useful to develop greater wellbore pressures. However, available evidence sugests that fractures rotated quickly and did not always "back-frac" to intersect the wellbore, and in this situation neither higher pump rates or the employment of viscous fracturing fluids are likely to be of benefit.

CONCLUSIONS

The following problems can be encountered in stress regimes where the least principal stress is vertical:

Horizontal fractures can be initiated at the wellbore as a result of fluid infiltration into the wellbore wall. The mechanism does not necessarily require the existence of bedding plane weakness or incipient macroscopic fractures. The most expedient remedy is to increase wellbore pressure to breakdown levels quickly, preferably in less than 10 sec. The employment of downhole pumps would be useful in this regard.

In situations where recorded ISIPs lie close to the estimated vertical stress, a demonstration that the fracture trace was vertical at the wellbore cannot be taken as proof that the ISIPs reflect least horizontal stress magnitudes.

An evaluation of the spatial variation of near-lithostic ISIPs in areas of rugged topography can be useful for distinguishing whether they reflect S_v and S_h, but is practicable only where data from multiple boreholes are available. Where data from only one borehole are available a conservative interpretation would be to accept near-lithostat ISIPs as placing only lower bounds on the true magnitude of S_h.

Vertical fractures induced in strongly (horizontal) bedded shale appear to have rotated to horizontal after propagating less than several wellbore diameters, but did not then cut back to intersect the wellbore.

The state of drainage of the induced fracture did not affect the observed ISIP.

There are as yet no foolproof methods for determining whether a near-lithostat ISIP reflects S_v or S_h from the form of the post-shut-in pressure decline.

When conducting measurements in regions where "thrust regime" conditions are anticipated, it is prudent to secure the capability of injecting fluid at rates significantly higher than 10 l/min to maximize the prospects of inflating any vertical fracture which may be co-existing with any horizontal fracture that intersects the wellbore. The employment of fracturing fluids more viscous than water may be advantageous in this regard. In order to recognize any subtle features in the resulting pressure decline curve following shut-in, which may be attributed to the closure of the vertical fracture, hydraulically stiff pressuring systems which isolate the fracturing interval from the "wellbore" have advantage.

Acknowledgements—Original data collection was supported under DoE Contract Number DE-AC21-83MC2033F with contributing support from Schlumberger-Doll Research, Exxon Production Research and Institutional (L-DGO) funds. TE acknowledges support from EPRI Contract Number RP 2556-24. Klaus Jacob and Chris Scholz reviewed the manuscript. L-DGO Contribution Number 4528.

REFERENCES

1. Roegiers J.-C., McLennan J. C. and Schultz L. D. *In situ* stress determinations in northeastern Ohio. *Proc. 23rd U.S. Symp. on Rock Mechanics*, University of California, Berkeley, Aug. 25–27 (1982).
2. Haimson B. C., Lee C. F. and Huang J. H. S. High horizontal stresses at Niagara Falls, their measurement, and the design of a new hydroelectric plant. *Rock Stress* (O. Stephansson, Ed.), pp. 615–624. Centek, Luleå, Sweden (1986).
3. Stephansson O. and Ångman P. Hydraulic fracturing stress measurements at Forsmark and Stidsvi in Sweden. *Bull. Geol. Soc. Finland* **58** (1–2), 307–33 (1986).
4. Rundle T. A., Singh M. H. and Baker C. H. *In situ* stress measurements in the Earth's crust in the eastern United States. Report NUREG/E1-1126, Nuclear Regulatory Commission (1985).
5. Baumgartner J. and Zoback M. Interpretation of hydraulic pressure–time records using interactive analysis methods: application to *in-situ* stress measurments at Moodus, Connecticut. *Pre-Conference Proc. of 2nd Int. Workshop on Hydraulic Fracturing Stress Measurements*, Minneapolis, June 15–18, pp. 619–645 (1989).
6. Haimson B. C. Hydraulic fracturing in porous and non-porous rock and its potential for determining *in situ* stresses at great depth. Ph.D. Thesis, University of Minnesota (1968).
7. Bjarnason B., Ljunggren C. and Stephansson O. New developments in hydrofracturing stress measurement technology at Luleå. *Pre-Conference Proc. of 2nd Int. Workshop on Hydraulic Fracturing Stress Measurements*, Minneapolis, June 15–18, pp. 113–140 (1989).
8. Kehle R. O. Determination of tectonic stresses through analysis of hydraulic well fracturing. *J. Geophys. Res.* **69**, 259–273 (1964).
9. Warren W. E. Packer-induced stresses during hydraulic fracturing. *J. Energy Resources Technol.* **103**, 336–343 (1981).
10. Evans K., Scholz C. and Engelder T. An analysis of horizontal fracture stress measurements in granite at North Conway, New Hampshire. *Geophys. J.* **93**, 251–264 (1988).
11. Hoag R. B. and Stewart G. W. Preliminary petrographic and geophysical interpretations of the exploratory geothermal drill hole and core, Redstone, New Hampshire. Report prepared for U.S. ERDA under contract number EY-76-S-02-2720, Dept of Earth Science, University of New Hampshire, Durham (1977).
12. Evans K. F. A laboratory study of two straddle-packer systems under simulated hydrofrac stress-measurement conditions. *J. Energy Resources Technol.* **109**, 180–190 (1987).
13. Rice J. R. and Cleary M. P. Some basic stress diffusion solutions for fluid-saturated elastic porous media with compressible constituents. *Rev. Geophys. Space Phys.* **14**, 227–241 (1976).
14. Jaeger J. C. Extension failures in rocks subject to fluid pressure. *J. Geophys. Res.* **68**, 6066–6067 (1963).
15. Hubbert M. K. and Willis D. G. Mechanics of hydraulic fracturing. *Trans. Am. Inst. Min. Engrs* **210**, 153–158 (1957).
16. Jaeger J. C. and Cook N. G. W. *Fundamentals of Rock Mechanics*, 2nd Edn, *Science Paperbacks No. 12*. Wiley, New York (1976).
17. Enever J. Ten years experience with hydrofracture fracture stress measurements in Australia. *Pre-Conference Proc. of 2nd Int. Workshop on Hydraulic Fracturing Stress Measurements*, Minneapolis, June 15–18, pp. 1–93 (1989).

18. Zoback M. D., Healy J. H. and Roller J. C. Preliminary stress measurements in Central California using the hydraulic fracturing technique. *Pure Appl. Geophys.* **115,** 135–152 (1977).
19. Warren W. E. and Smith C. W. *In situ* stress estimates from hydraulic fracturing and direct observation of crack orientation. *J. Geophys. Res.* **90,** 6829–6839 (1985).
20. Evans K. F., Engelder T. and Plumb R. A. Appalachian stress study 1: a detailed description of *in situ* stress variations in Devonian shales of the Appalachian Plateau. *J. Geophys. Res.* **94,** 7129–7154 (1989).
21. Evans K. F. and Engelder T. Measurement and study of stress variations within the Appalachian basin of western New York. *Proc. Unconventional Gas Recovery Contractor's Meeting*, Morgantown, WV, Nov 18–19. NTIS publication number DOE/METC-86/6034 (1985).
22. Savage W. Z., Swolfs H. S. and Powers P. S. Gravitational stresses in long symmetric ridges and valleys. *Int. J. Rock Mech. Min. Sci. & Geomech. Abstr.* **22,** 291–302 (1985).
23. Sturgul J. R., Scheidegger A. E. and Grinshpan Z. Finite element modeling of a mountain massif. *Geology* **4,** 439–442 (1976).
24. Bauer S. J., Holland J. F. and Parrish D. K. Implications about *in situ* stress at Yucca Mountain. *Proc. 26th U.S. Symp. on Rock Mechanics*, Rapid City, SD, 26–28 June (1985).
25. Evans K. F., Oertel G. and Engelder T. Appalachian stress study 2: analysis of Devonian shale core samples; implications for the nature of contemporary stress variations and Alleghanian deformation. *J. Geophys. Res.* **94,** 7155–7170 (1989).

APPENDIX

Modelling Stresses Due to Topography in the Study Area

The model is based on a plane strain solution for the stresses due to gravity in an idealized elastic medium that is a half-space in all respects other than the presence of a symmetric valley [22]. A form of topographic profile is assumed which is conformal under transformation to the half-plane. The "steepness" of the profile is determined by specifying the plateau height b above valley bottom and the distance from the valley centre to the point at which the elevation increase has reached one half the final plateau height. The degree to which the 2-D model represents the 3-D topography in the study area can be judged from Fig. 3 where we highlight in light and heavy stipple, ground above the 579 m (1900 ft) and 671 m (2200 ft) contours, respectively. Short wavelength contour variations such as from minor stream valleys are smoothed. The plateau top corresponds to the heavily-stippled area and the valley floor is taken as 457 m (1500 ft) amsl. Hence b is 213 m. Smoothed profiles in the immediate vicinity of the Wilkins and Appleton wells are shown in Fig. 3 together with the distance to the point where half the final plateau height is realized.

Two of the model profiles considered by Savage *et al.* [22] (cases $a/b = 2$ and 3) are relevant here, and for clarity we adapted their non-dimensionalized figures to the S. Canisteo situation by scaling them for a plateau height b of 213 m, and an overburden density ρ of 2.71 g/cm^3. The degree to which the model profiles represent estimated smooth topography near each well can be judged from Fig. 3. Contours of horizontal (left figures) and vertical (right figures) stress predicted for each of the two model profiles are shown in Fig. 7 (the figures differ from those presented by Savage *et al.* [22] in that a contour plotting error has been corrected). Each well is shown in its precise location and the traces are marked with graduations which denote the horizontal and vertical stresses that would be predicted for a gravitating, laterally confined, *half-space* model ($\nu = 1/3$) with the free-surface located at each specific wellhead [i.e. the overburden for the right plots and $\nu/(1-\nu)$ times this for the left]. All stresses are normalized to $\rho g b$, where b is the height of the plateau above the valley floor and hence the values shown must be multiplied by 5.66 MPa to obtain the true stress magnitudes.